

Experiments on power optimization for displacement-constrained operation of a vibration energy harvester

Binh Duc Truong, Cuong Phu Le and Einar Halvorsen

Department of Micro- and Nanosystem Technology, Buskerud and Vestfold University College, Campus Vestfold, Raveien 215, 3184 Borre, Norway

E-mail: Einar.Halvorsen@hbv.no

Abstract. This paper presents experiments on how to approach the physical limits on power from vibration energy harvesting under displacement-constrained operation. A MEMS electrostatic vibration energy harvester with voltage-control of the system stiffness is used for this purpose. The power saturation problem, when the proof mass displacement reaches maximum amplitude for sufficient acceleration amplitude, is shifted to higher accelerations by use of load optimization and tunable electromechanical coupling k^2 . Measurement results show that harvested power can be made to follow the optimal velocity-damped generator also for a range of accelerations that implies displacement constraints. Comparing to the saturated power, the power increases 1.5 times with the optimal load and an electromechanical coupling $k^2=8.7\%$. This value is 2.3 times for a higher coupling $k^2=17.9\%$. The obtained system effectiveness is beyond 60% under the optimization. This work also shows a first demonstration of reaching optimal power in the intermediate acceleration-range between the two extremes of maximum efficiency and maximum power transfer.

1. Introduction

Microelectromechanical systems (MEMS) vibration energy harvesting (VEH) is a potential approach to autonomously supply power for wireless sensors. When the harvested power is sufficient to operate the electronic system, use of inconvenient batteries can be eliminated. A typical VEH design is a spring-mass system. The proof mass motion induced by ambient vibrations leads to energy conversion based on either of three basic mechanisms: piezoelectric, electromagnetic and electrostatic [1, 2]. For low-loss resonant harvesters at the microscale, displacement-constrained operation is easily encountered because of the limited space available on chip. Beyond a critical acceleration sufficient to drive the proof mass displacement to its maximum amplitude, the power is saturated [3, 4] and left increasingly far below the theoretical power bound for displacement-limited operation [5]. This bound is conservatively approximated by the optimal velocity-damped generator (VDRG) whose power increases linearly with acceleration. The question is therefore how to avoid saturation and further improve power for acceleration amplitudes beyond the critical value? Utilization of transducing end-stops in our previous impact-device concept [6] somewhat overcomes this problem, but it demands complex optimization of the device design to further increase power in the impact regime. In addition, for a two-port harvester operating under displacement-constrained operation it has been shown that



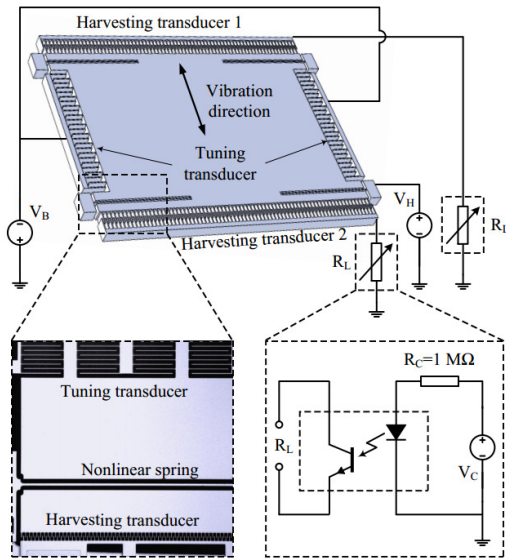


Figure 1. Key features of the device design, sketch of the electrical setup with the load tuning control. A close-up view of device fabricated using the SOIMUMPS process with the device layer thickness of $t = 25 \mu\text{m}$.

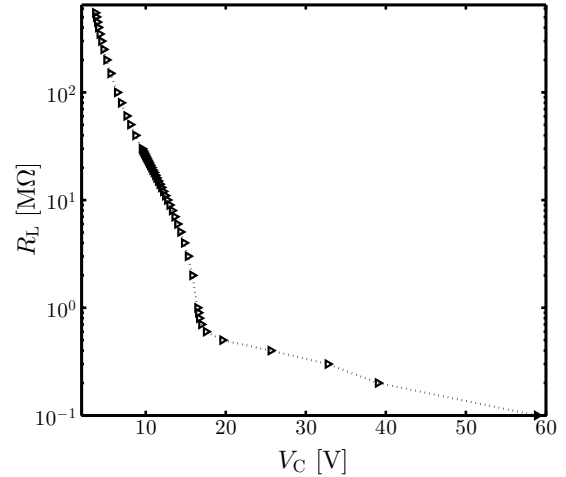


Figure 2. Characterization of the opto-coupling resistor under driving of the voltage source V_C .

it is ultimately optimal to maximize efficiency [7] which is equivalent to maximizing electrical damping. Hence, maximum efficiency and maximum power transfer (unconstrained motion) constitute two extremes, but the intermediate optimization cases have not been studied.

In this work, we investigate an approach to optimize power in both damping-limited regime and displacement-limited regime. Harvester power is then maximized in the intermediate range. The approach is motivated by electrical damping being the control parameter in optimization of the VDRG [2]. We here consider load-resistance optimization and adjustment of the electromechanical coupling. Both these factors directly affect the electric damping and are used to keep the displacement amplitude at the limit for the VDRG. It should be noted that a resistive load such as we use here can emulate a buck-boost converter that has no input filter capacitor [8]. It is therefore much more than an experimental convenience. For the experiments we employ a previous large-frequency-tuning-range resonator device [9] as a MEMS electrostatic vibration energy harvester. The system stiffness and the electromechanical coupling can be adjusted by an applied voltage. This, together with an electrically controllable load resistance let us explore the optimization problem.

2. MEMS device

Figure 1 shows key features of the electrostatic device. The harvesting transducers are two anti-phase comb-drive capacitance structures with a nominal capacitance $C_0=0.47 \text{ pF}$. The proof mass is suspended by four single beams. The restoring force is designed to have hardening nonlinearity. The device stiffness is tuned by a bias control $V_T=V_H+V_B$ of the tuning transducer which is a gap-closing capacitor structure. When the electrodes of the harvesting transducers are short-circuited, the net force is approximated by

$$F_{\text{net}}(x) = (k_m - \frac{C_T}{g^2} V_T^2)x + (\frac{k_m}{l^2} - \frac{2C_T}{g^4} V_T^2)x^3 \quad (1)$$

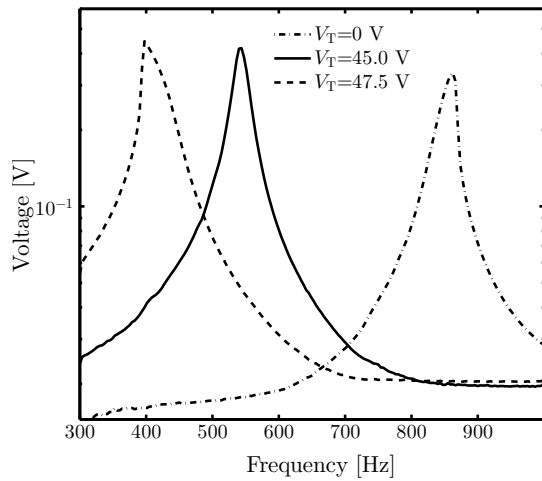


Figure 3. Measured frequency responses for increase of the tuning voltage V_T at a small acceleration $A=0.21$ g and the load $R_L=20$ M Ω .

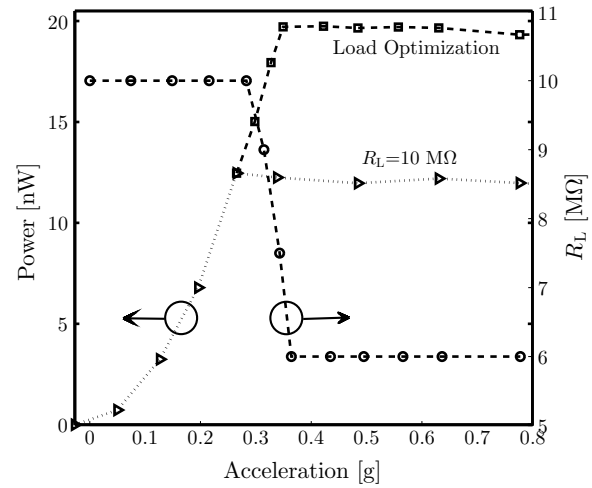


Figure 4. Measured power in damping-limited regime and displacement-limited regime with corresponding optimal load for $V_T=45.0$ V.

where k_m is the linear stiffness of the restoring force, $l=\sqrt{\frac{735}{512}}w$, w is the beam width, g and C_T are the nominal gap and the nominal capacitance of the tuning transducer. The generated power is obtained by connection of the fixed-electrode of the harvesting transducers to the variable load R_L . To avoid cumbersome resistor changes, the load used in the experiment is the opto-coupling resistor V0617A with low coupling capacitance. The load value R_L is set by a voltage V_C and a series resistance R_C . Figure 1 also displays a close-up view of the device, which is fabricated using the SOIMUMPS process with a device layer thickness of $t=25$ μm . The nonlinear spring and a part of all transducers are shown in the optical micrograph. By design, the maximum amplitude of the proof mass displacement $X_{\text{max}}=5.5$ μm is defined by rigid end-stops. Further details of the device parameters can be found in [9].

3. Measurements

The opto-coupling resistor is characterized under control of the voltage V_C and a series resistance $R_C=1$ M Ω as shown in figure 2. The optical coupling between the diode emitter and the phototransistor leads to the variable resistance that is high at low V_C and vice-versa. The load can be adjusted from 500 M Ω down to 100 K Ω when V_C varies from 3.7 V to 58.9 V. This characterization is used in all measurements of the device. The bias voltage for the harvesting transducers is chosen as $V_H=45.0$ V. Figure 3 shows the measured frequency responses at the small acceleration regime when the proof mass displacement is still below the limit X_{max} . The hardening effect due to the nonlinear spring is evident for $V_T=0.0$ V with a center frequency 831.5 Hz. The effective stiffness of the system reduces with increase of the bias V_T of the tuning transducer, giving higher output voltages and lower center frequencies. The system response is roughly linear for $V_T=45.0$ V, which gives a center frequency $f_c=531.5$ Hz. The device exhibits softening effects for $V_T=47.5$ V. The critical voltage that causes pull-in instability is estimated to $V_{\text{cr}} \sim 50$ V. We now use $V_T = 45.0$ V as a case for load optimization in both the damping-limited regime and the displacement-limited regime.

Figure 4 shows measured powers and corresponding optimal load for each RMS acceleration amplitude at the center frequency f_c . In the damping-limited regime, the optimal load is $R_L=10$ M Ω in this case. Keeping this resistance while varying the acceleration, the power saturates at

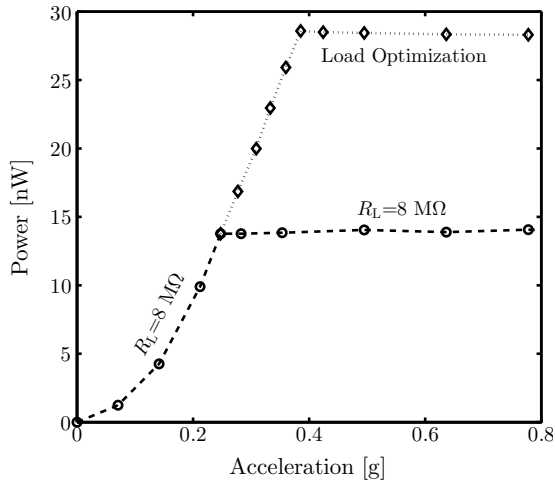


Figure 5. Measured power both with and without load optimization for $V_T=47.5$ V.

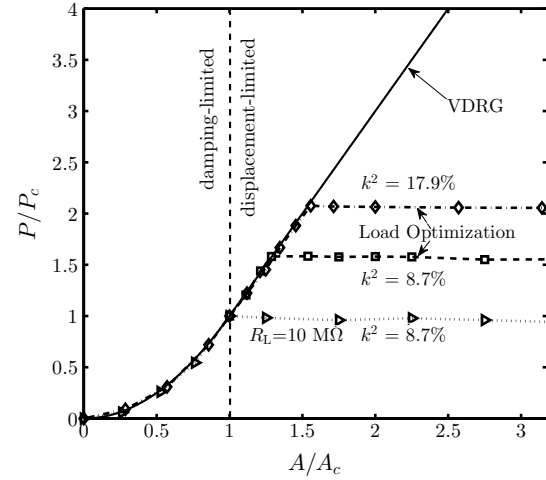


Figure 6. Comparison of the maximum power to the optimal velocity-damped generator VDRG for $k^2 = 8.7\%$ ($V_T=45.0$ V) and $k^2 = 17.9\%$ ($V_T=47.5$ V).

$P_c=12.4$ nW for accelerations larger than a critical value $A_c=0.28$ g. We interpret this as the proof mass displacement reaching the maximum X_{\max} at A_c and that it hits the end-stops for $A > A_c$. However, the power can be improved for $A > A_c$ by adjusting the load separately for every acceleration amplitude. The measured result shows that the power can be improved for acceleration amplitudes between $A > A_c$ and 0.36 g where the power looks approximately linear in A . For $A > 0.36$ g the power saturates at 19.7 nW. All corresponding optimal loads and accelerations can be found in figure 4. The optimal load only varies between A_c and 0.36 g and is again constant for $A > 0.36$ g. Note that no attempt is made to avoid proof mass impacts on the end-stops. Therefore the power-acceleration curve here is significantly different from the theoretical result in [5]. It is reasonable to interpret the optimized value $R_L=6.0$ M Ω as the resistance value that gives maximum electrical damping. Increase of the tuning voltage V_T leads to a reduced net stiffness and higher electromechanical coupling k^2 . This is advantageous to further increase the harvested power under displacement-constrained operation. Figure 5 shows the measured power for $V_T=47.5$ V when driven at the center frequency $f_c=400.0$ Hz. The device now reaches a higher critical power of $P_c=13.8$ nW at a lower $A_c=0.25$ g, compared to the previous case of $V_T=45.0$ V. With load optimization for $A > A_c$, the power continues to increase to a maximum of 28.6 nW at $A=0.38$ g. This power about 1.5 times better than the previous case.

In the linear approximation, the anti-phase comb-drive harvesting transducers are equivalently converted to a two-port model because of decoupling of the common and differential modes [10, 11]. For a displacement-limited two-port device, one can show that load optimization can boost the harvested power to a maximum value of

$$P_{\max} \approx \frac{1}{2} k^2 Q_m P_c \quad (2)$$

where the mechanical quality factor Q_m is estimated from the full bandwidth at half maximum of the open-circuit frequency response and k^2 is the electromechanical coupling of the linear two-port model, evaluated by

$$k^2 = 1 - \frac{f_r^2}{f_{\text{ar}}^2} \quad (3)$$

Table 1. Measured electromechanical coupling factor and figure of merit k^2Q_m at $A=0.03$ g.

Tuning voltage	Electromechanical coupling k^2	k^2Q_m
$V_T= 45.0$ V	8.7%	3.2
$V_T= 47.5$ V	17.9%	4.7

where f_r is the resonant frequency measured with short-circuited output and f_{ar} is the resonant frequency measured with open-circuited output. Table 1 shows the measured coupling k^2 and a corresponding figure of merit k^2Q_m . The achieved power is compared to the maximum possible power of the optimal velocity-damped generator under displacement-constrained operation in figure 6. The power and the acceleration are normalized by the factors P_c and A_c respectively because P/P_c is a universal function of A/A_c for all VDRGs. The comparison in the damping-limited regime shows that the power obtained with load optimization closely approaches the optimal VDRG up to a maximum acceleration beyond A_c . In the displacement-limited regime, the range of accelerations where the optimum can be followed depends on k^2Q_m as is seen by comparing the maximum power $1.54P_c$ at $A=1.28A_c$ for $k^2=8.7\%$ to the maximum power $2.07P_c$ at $A=1.55A_c$ for $k^2=17.9\%$. The corresponding estimates of maximum power from (2) are respectively $1.6P_c$ and $2.4P_c$ giving best correspondence with the lowest-coupling configuration which is also the most linear one. It is noteworthy that even though the high-coupling configuration exhibited clear softening nonlinearities, it follows the optimal VDRG curve as closely as the other alternative until its maximum is reached.

4. Conclusion

Electrical damping is controlled through load resistance and electromechanical coupling to maximize power for a vibration energy harvester under displacement-constrained operation. The measured power closely follows the optimal VDRG even between the two extremes of unconstrained proof mass motion and displacement-limited operation with saturated power. The load optimization makes a gradual transition between these two extremes which we can think of respectively as maximum power-transfer and maximum efficiency. For displacement-limited operation, there are significant improvements in power from increasing electromechanical coupling even for a high-coupling device.

Acknowledgment

This work was supported by the Research Council of Norway through Grant no. 229716/E20.

References

- [1] T. Starner, *IBM Systems J.*, **35** 618 (1996)
- [2] P. D. Mitcheson et. al., *Proceedings of the IEEE*, **96** 1457 (2008)
- [3] M. S. M. Soliman et. al., *J. Micromech. Microeng.*, **18** 115021 (2008)
- [4] D. Hoffmann, B. Folkmer and Y. Manoli, *J. Micromech. Microeng.*, **19** 094001 (2009)
- [5] E. Halvorsen et al., *J. Phys.: Conf. Ser.* **476** 012026 (2013)
- [6] C. P. Le, E. Halvorsen, Søråsen O and Yeatman E M, *J. of Int. Mat. Syst. Struc.*, **23** 1409 (2012)
- [7] M. Renaud et. al., *J. Micromech. Microeng.*, **22** 105030 (2012)
- [8] R. D'hulst, T. Sterken, R. Puers, G. Deconinck and J. Driesen, *IEEE Trans. Indust. Electro.*, **57** 4170 (2010)
- [9] C. P. Le and E. Halvorsen, *Proceedings of the Transducers & Eurosensors XXVII*, 1352 (2013)
- [10] F. Peano and T. Tambosso, *J. Microelectromech. Syst.*, **14** 429 (2005)
- [11] H. A. C. Tilmans, *J. Micromech. Microeng.*, **6** 157 (1996)